



RAPID COMMUNICATION

Neutralization of SARS-CoV-2 infection by antibodies targeting diverse epitopes

The COVID-19 pandemic that started in late 2019 is sweeping through the world, posing historic challenges to global health, and disrupting social and economic lives. Previous and recent studies indicate that monoclonal antibodies can be efficacious in preventing and treating SARS-CoV-1 and SARS-CoV-2 infections. Using a phage display platform, we have identified dozens of monoclonal antibodies that bind to diverse epitope groups on the SARS-CoV-2 spike protein. Many of them bound to the receptor binding domain (RBD) and inhibited ACE2-RBD interaction. Several of them were capable of inhibiting SARS-CoV-2 spike protein pseudo-typed virus (pseudovirus) entry. In addition, we isolated a dozen of S2 binding antibodies that prevented pseudovirus entry without inhibiting the ACE2-RBD interaction. A bi-epitopic antibody constructed from two non-competing, RBD binding, neutralizing antibodies displayed higher potency than either of them alone. Combinations of RBD and S2 binding antibodies displayed additive inhibitory effects against pseudovirus infection. The new antibodies and strategies reported here could expand the arsenal of anti-COVID-19 therapeutics and help understand the viral entry mechanism, the pathogenesis of the SARS-CoV-2, and anti-SARS-CoV-2 vaccine development.

Panning was performed using three different SARS-CoV-2 related antigens including RBD, S1, the spike ectodomain, and two control antigens (RSV F protein and Siglec-15), against both IgG and IgM libraries. Among antibodies against SARS-CoV-2, the Vh3-30, Vh3-23, Vh1-69, and Vh6-1 were frequently used (Fig. S1A, C). Vh1-69 was more frequently used by a large number of neutralizing antibodies against respiratory tract infections such as influenza and other viruses.¹ It is interesting to note that a good number of leads were generated from both IgG and IgM libraries for all three antigens, even though the percentage of IgG library-derived leads appears to be slightly higher against RSV than against the other two antigens (Fig. S1B). There are statistically higher mutational rates associated

with leads derived from the IgG library than from the IgM library for each of the panning antigens. Furthermore, leads derived from the IgG library against RSV and SARS-CoV-2 had higher mutational rates than those against Siglec-15 (Fig. S1D).

In an initial single-point competition ELISA screening, when evaluated in the scFv-Fc format, the majority of the RBD binders displayed moderate to high inhibitory activities against RBD-ACE2 interaction with 50% of them inhibiting more than 60% (Fig. 1A). The inhibitory dose-response curves exhibited different inhibition patterns (Fig. 1B), suggesting different affinities or epitope usages. The most potent antibodies were converted to IgG and their inhibitory activity against RBD-ACE2 interaction was confirmed by both ELISA- and cell-based competition assays (Fig. 1C, D). Their KDs are mostly in the range of single digit nM (Fig. 1E). In an epitope binning experiment, RBD-35 occupied an epitope that was distinct from those of RBD-32 and 18, even though they all competed with ACE2 for binding to RBD (Fig. 1F). In line with the RBD-ACE2 interaction inhibition assay, RBD-35 was the most potent neutralizing antibody. Although RBD-32 and RBD-18 showed similar activity in competing with RBD to bind to ACE2, RBD-32 was much more potent than RBD-18 in our pseudovirus assay (Fig. 1G). Besides, RBD-35, RBD-32, and RBD-18 were the 3 out of 32 tested antibodies in scFv-Fc format that showed cross-reactivity to SARS-CoV-1, but their cross-activities were generally weaker than to SARS-CoV-2 (Fig. S2A, B). Only RBD-32 retained cross-activity after being converted to IgG, both against S1 (Fig. S2C) and RBD (Fig. S2D). RBD-32 showed a potency similar to ACE2-Fc in our SARS-CoV-1 pseudovirus assay (Fig. 1H). Antibody RBD-35 showed good activity against D614G, Alpha, and Cluster 5, moderate activity against Beta, Gamma, and Omicron, and lost activity against Delta (Fig. 1I).

The combination of two or even more antibodies is a proven strategy to improve the therapeutic efficacies against infectious diseases. We constructed a bi-specific antibody with RBD-35 IgG as the foundation and attached RBD-32 scFv to the C-termini of the heavy chain (Fig. 1J).

Peer review under responsibility of Chongqing Medical University.

<https://doi.org/10.1016/j.gendis.2023.101088>

2352-3042/© 2023 The Authors. Publishing services by Elsevier B.V. on behalf of KeAi Communications Co., Ltd. This is an open access article under the CC BY-NC-ND license (<http://creativecommons.org/licenses/by-nc-nd/4.0/>).

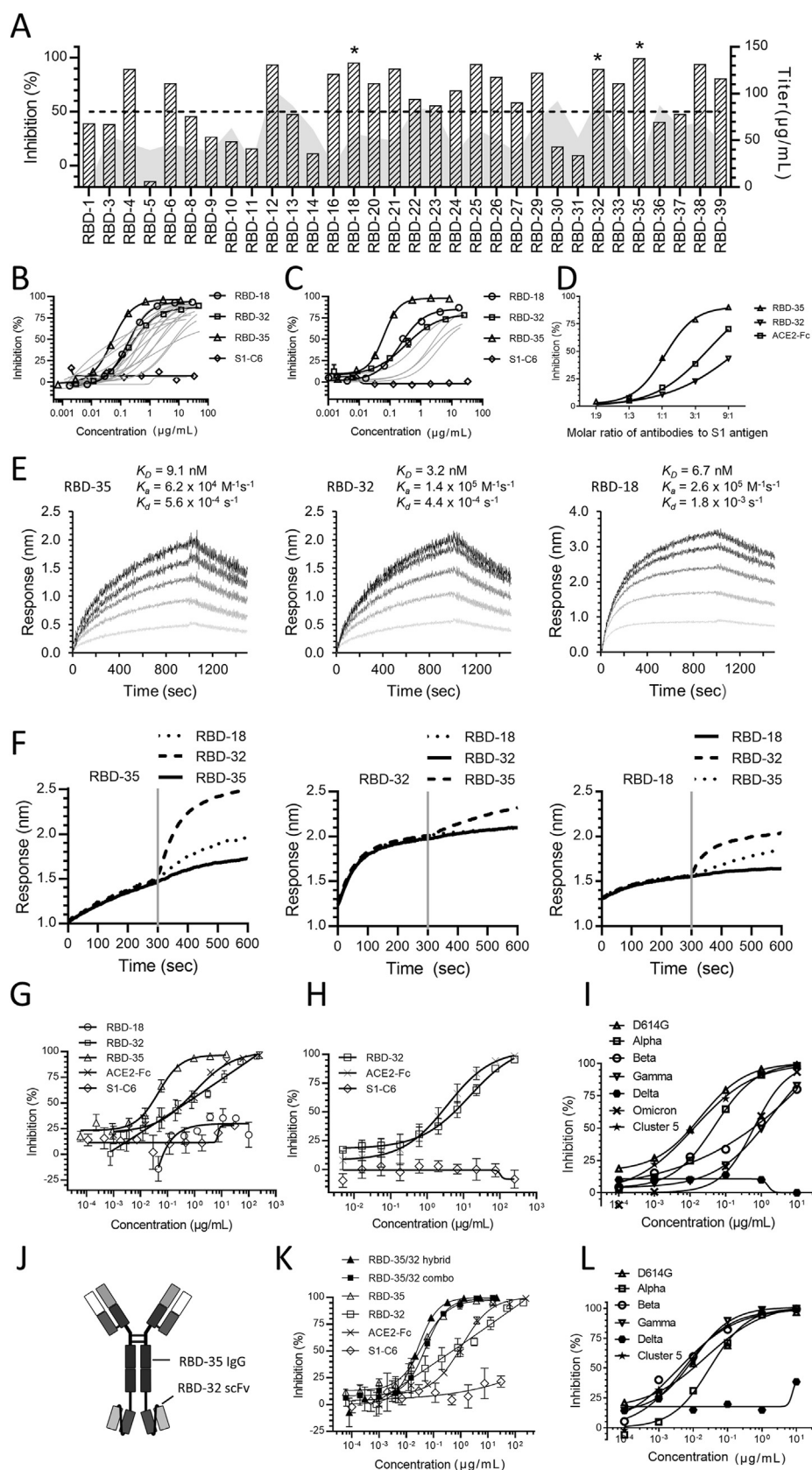


Figure 1 Identification of RBD binders. **(A)** Screening of antibodies in scFv-Fc format that inhibit RBD-ACE2 interactions by a single-point competitive ELISA. The competitive ELISA was performed by preincubating a 1:8 diluted sample with 5 ng/mL biotinylated RBD, followed by adding it to the ACE2-Fc coated plate. The titers of neat samples are shown by a curve with shaded areas.

This bi-epitopic antibody displayed significantly improved KD over their parental antibodies (Fig. S3A) and exhibited similar inhibition against RBD-ACE2 interaction compared with RBD-35 (Fig. S3B). Importantly, this hybrid antibody showed at least a three-fold improvement in pseudovirus neutralization against SARS-CoV-2 over RBD-35 (Fig. 1K). The RBD-35 and -32 combo, on the other hand, only displayed additive effects. The anti-SARS-CoV-1 neutralizing ability of RBD-32 is only partially endowed to this hybrid molecule (Fig. S3C) perhaps due to the structural constraint on RBD-32 in the bi-epitopic configuration. In the aspect of neutralizing SARS-CoV-2 variants, RBD-35/32 hybrid showed excellent activity against D614G, Alpha, Beta, Gamma, Cluster 5 Deltacron, and Omicron but Delta (Fig. 1L). To further validate the neutralizing capability of the antibodies in neutralizing SARS-CoV-2 Variants, Vero E6 cells were used in neutralization assays. The neutralizing activity of R35 and R35-32 antibodies in blocking SARS-CoV-2 variants infection of Vero E6 cells was consistent with that of ACE2-HEK293T cells (Fig. S4A, B). Some studies have shown that neutralizing antibodies may lose their effectiveness against the Delta variant. This could be due to their high sensitivity to the L452R mutation, which is commonly found in the Delta variant. As a result, the presence of the L452R mutation likely reduces the neutralizing activity of antibodies such as R35 and R35-32.

There remains a question as to whether antibodies targeting the S2 region possess neutralizing activities and therapeutic value.² The S2 binders account for nearly half of all ectodomain binders derived from ectodomain panning (Fig. S5A, B). Contrary to the RBD binders, the majority of the S2 binders displayed strong cross-reactivity against the SARS-CoV-1 ectodomain (Fig. S5C). In a single-point pseudovirus neutralization screening against both SARS-CoV-1 and SARS-CoV-2, many of the S2 binders displayed neutralizing ability against SARS-CoV-2, albeit potencies were rather moderate compared with some of the RBD binders (Fig. S5D). Some of the S2 binders also displayed modest neutralizing ability against the SARS-CoV-1 pseudotyped virus (Fig. S5E). Representative S2 binders from

the ectodomain campaign are converted to IgG for further analysis. After conversion, these S2 binders retained characteristics of their scFv-Fc counterparts in binding to the ectodomain and S2 domain (Fig. S6A, B). They also retained the cross-reactivity against SARS-CoV-1 (Fig. S6C) but failed to interfere with ectodomain-ACE2 interaction as expected (Fig. S6D). However, unlike the selected RBD binders, the selected S2 binders only partially inhibited the pseudovirus entry, even though they reached maximum inhibition at lower concentrations (Fig. S6E). We tested if S2 binders and RBD binders could cooperate in their neutralization against the SARS-CoV-2 pseudovirus. RBD-32 was chosen for this purpose due to its relatively weak neutralizing activity that may allow easier observation of any potential additive effect in the concentration ranges of antibodies used. Secto-40 and Secto-45 were chosen for their better inhibition profiles. Both Secto-40 and Secto-45 when combined with RBD-32 reached higher percentages of inhibition than either one alone in the pseudovirus neutralization assay (Fig. S7).

Using the phage display platform as an antibody discovery platform opened a new era in biologics discovery³ and contributed to several FDA-approved antibody therapeutics,⁴ especially the practice to generate naïve libraries from the IgM repertoire. In this study, we report the isolation of potent neutralizing antibodies targeting the RBD region. Moreover, we found that bi-epitopic antibodies constructed from two non-competing antibodies offer better protection against pseudovirus infection than either of the parental antibodies alone, suggesting a new way of improving anti-viral potency, prevention of viral escape, and more convenient process development. We also present data from a large collection of S2-binding antibodies. S2 is another functional domain of the SARS-CoV-2 spike protein and plays an important role in the virus infection process. Neutralizing peptide targeting S2 heptad repeat region was reported recently.⁵ It will be important to further evaluate the RBD targeting and the S2 targeting antibodies in preventing and treating SARS-CoV-2 infection in more clinically relevant settings.

(B) Dose-response curves of selected samples from the single-point ELISA screening. Leads with promising IC₅₀, maximum inhibition efficiencies, and dose-response slopes are highlighted in bold lines. S1–C6, which binds to the SD1 region of the SARS-CoV-2 spike protein, was used as the negative control. **(C)** Dose-response curves of RBD binders in IgG format after being converted from selected antibodies in the scFv-Fc format as measured by ELISA. S1–C6 in IgG format was used as the negative control. **(D)** HEK 293T cells were overexpressed with ACE2 on the surface and used for testing the antigen competition. Recombinant ACE2-Fc protein was used as a control. **(E)** Biolayer interferometry analysis of lead antibodies in IgG format. The binding profile was determined by immobilizing a tested antibody onto anti-Fc capture (AHC) biosensors from ForteBio, followed by dipping the loaded probes into a series of concentrations of RBD-SD1. The applied antigen concentrations were 6.25 nM, 12.5 nM, 25 nM, 50 nM, and 100 nM. The binding affinities and the kinetic parameters were calculated based on the global fitting of the data using a 1:1 binding model. **(F)** In-tandem epitope binning of selected leads in IgG format. To perform the binning assay, streptavidin probes were first loaded with biotinylated RBD protein, followed by the binding of the saturated testing antibody and competing antibody sequentially. **(G–I)** Dose-response curves of leading RBD antibodies in neutralizing SARS-CoV-2 spike protein pseudotyped virus (G), SARS-CoV-1 spike protein pseudotyped virus (H), and SARS-CoV-2 spike protein pseudotyped variants (I). **(J)** The schematic diagram of the RBD-35/32 hybrid antibody in which RBD-32 scFv is attached to the C-terminus of the RBD-35 heavy chain through a flexible linker (GGGGS)₃. **(K)** Neutralizing activities of the RBD-35/32 hybrid antibody in comparison with those of the RBD-35/32 combo, RBD-35, RBD-32, and ACE2-Fc in SARS-CoV-2 pseudovirus assays. S1–C6 was used as a negative control. Error bars = STD. The data are average values of triplicates from a single experiment. **(L)** Neutralizing activities of the RBD-35/32 hybrid antibody against SARS-CoV-2 variants. The data are displayed as mean ± SD from duplicates.

Author contributions

SW, HM, KY, YL, ZS, HH, LZ, JZ, HC, and AW conducted most of the experiments and drafted the manuscript. HY and YB contributed to technical and administrative assistance. LH, HJ, XX, YX, YY, and JZ analyzed and interpreted results, participated in critical discussions, and edited the manuscript. JZ was responsible for financial support.

Conflict of interests

The authors SW, YX, HJ, and JZ are employees of Jecho Laboratories Inc. and hold patents on the antibodies described in this manuscript.

Funding

This work was funded by the National Natural Science Foundation of China (No. 81773621, 82073751 to JZ), the National Science and Technology Major Project "Key New Drug Creation and Manufacturing Program" of China (No. 2019ZX09732001-019 to JZ), the Key R&D Supporting Program (Special support for developing medicine for infectious diseases) from the Administration of Chinese and Singapore Tianjin Eco-city to Jecho Biopharmaceuticals Ltd. Co., Zhejiang University special COVID-19 grant 2020XGZX099, and Shanghai Jiao Tong University "Crossing Medical and Engineering" grant 20X190020003 to JZ.

Acknowledgements

The following reagent was obtained through BEI Resources, NIAID, NIH: NR-52511, *Homo sapiens* human embryonic kidney cells (HEK-293T) expressing human angiotensin-converting enzyme 2, HEK-293T-hACE2 cell line.

Appendix A. Supplementary data

Supplementary data to this article can be found online at <https://doi.org/10.1016/j.gendis.2023.101088>.

References

1. Chen F, Tzarum N, Wilson IA, Law M. VH1-69 antiviral broadly neutralizing antibodies: genetics, structures, and relevance to rational vaccine design. *Curr Opin Virol*. 2019;34:149–159.
2. Liu L, Wang P, Nair MS, et al. Potent neutralizing antibodies against multiple epitopes on SARS-CoV-2 spike. *Nature*. 2020; 584(7821):450–456.
3. Marks JD, Hoogenboom HR, Bonnert TP, McCafferty J, Griffiths AD, Winter G. By-passing immunization. Human antibodies from V-gene libraries displayed on phage. *J Mol Biol*. 1991;222(3):581–597.
4. Frenzel A, Schirrmann T, Hust M. Phage display-derived human antibodies in clinical development and therapy. *mAbs*. 2016; 8(7):1177–1194.
5. Xia S, Liu M, Wang C, et al. Inhibition of SARS-CoV-2 (previously 2019-nCoV) infection by a highly potent pan-coronavirus fusion inhibitor targeting its spike protein that harbors a high capacity to mediate membrane fusion. *Cell Res*. 2020;30(4):343–355.

Shusheng Wang ^{a,b,1}, Yunji Liao ^{a,1}, Kaiyong Yang ^{b,1}, Hang Ma ^{a,1}, Zhangyi Song ^b, Haiqiu Huang ^b, Li Zhang ^b, Ailing Wang ^b, Lei Han ^c, Jiawei Zhang ^a, Hui Chen ^a, Haiyang Yin ^a, Yanlin Bian ^a, Hua Jiang ^{b,**}, Xiaodong Xiao ^b, Yueqing Xie ^b, Yunsheng Yuan ^{a,***}, Jianwei Zhu ^{a,b,*}
^aEngineering Research Center of Cell and Therapeutic Antibody, Ministry of Education, School of Pharmacy, Shanghai Jiao Tong University, Shanghai 200240, China
^bJecho Laboratories, Inc., Frederick, MD 21704, USA
^cJecho Institute Co., Ltd., Shanghai 200240, China

*Corresponding author. Engineering Research Center of Cell and Therapeutic Antibody, Ministry of Education, School of Pharmacy, Shanghai Jiao Tong University, 800 Dongchuan Road, Shanghai 200240, China.

**Corresponding author.

***Corresponding author.

E-mail addresses: hua.jiang@jechohabs.com (H. Jiang), yunsheng@sjtu.edu.cn (Y. Yuan), jianweiz@sjtu.edu.cn (J. Zhu)

11 November 2022

Available online 9 September 2023

¹ These authors contributed equally to this work and shared the first authorship.